ISSN 0915-633X

NATIONAL INSTITUTE FOR FUSION SCIENCE

Effect of Argon Additive in Negative Hydrogen Ion Sources

M. Bacal, M. Nishiura, M. Sasao, M. Wada,
M. Hamabe and H. Yamaoka

(Received - July 17, 2001)

NIFS-711 Aug. 2001

RESEARCH REPORT
NIFS Series

TOKI, JAPAN

Effect of argon additive in negative hydrogen ion sources*

M. Bacal#, M. Nishiura##, M. Sasao, M. Wada[1], M. Hamabe, H. Yamaoka[2],

National Institute for Fusion Science, Oroshi, Toki, Gifu-509-5292, Japan
[1] Doshisha University, Kyotanabe, Kyoto 610-0321, Japan
[2] Harima Institute, RIKEN, Hyogo, 679-5148, Japan

Abstract

We investigated using the photodetachment technique the negative ion density in the extraction region of a magnetically filtered multicusp ion source (21 cm in diameter and 27 cm long) when argon is added to hydrogen (up to 100%). A cylindrical probe was used to measure the plasma parameters (electron density and temperature, plasma and floating potential). We found that the negative ion density goes up at most by a factor 1.5 when argon is added to low base hydrogen pressure (0.05 or 0.1 Pa), but goes down when argon is added to higher initial hydrogen pressure (0.5 or 1 Pa). The optimum argon additive pressure is 40 to 60% of the base hydrogen pressure. The replacement of hydrogen by argon when the total pressure is kept constant does not change the electron temperature. We found that the negative ion temperature is lowered by the argon mixing to hydrogen. We also checked the hypothesis proposed by Curran *et al* [1], namely that the sequential energy transfer from the excited argon states through a photon to hydrogen singlet states would be the cause of enhanced highly excited vibrational population of hydrogen molecules. To do this we investigated whether the argon additive had any effect on the Werner and Lyman system lines in the VUV . No effect of argon on the mentioned hydrogen lines was found .

Keywords

Negative ions, H^-, vibrational excited molecules, argon additive, Werner system, Lyman system, VUV, Photo detachment

---

* Summary of work effected during the visit to NIFS of M. Bacal from September 15 to December 15, 2000.

Permanent address : LPTP, Ecole Polytechnique, 91128 Palaiseau, France

Present address : Beam Physics Laboratory, Wako-Institute, RIKEN, Saitama 351-0198, Japan

Introduction.

This work was initiated following the publication during this year of three articles [1−3] in which the addition of argon to hydrogen was described as beneficial for the hydrogen negative ion density [1] or for the extracted negative ion current [2,3].

Curran et al [1] studied the effect of helium, neon, argon and xenon additives on the production of negative hydrogen ions in a magnetically confined dc filament discharge. The addition of helium and neon produces effects not significantly different from an equivalent increase in hydrogen pressure. However, the addition of argon and low fractions of xenon produces significant increases in the negative-ion density for hydrogen pressures close to 0.133 Pa. The mentioned authors claim that the addition of argon and xenon, by increasing the electron density and decreasing the electron temperature, achieves conditions closer to optimum for negative-ion production. It is suggested in [1] that in the case of argon, when the largest enhancement occurs (a factor of 3, when 20% to 40% of argon is added), a resonant energy exchange between excited argon atoms and hydrogen molecules is a contributing factor. This is due, according to Curran *et al*, to the fact that argon has excited states with energies very close to those of the vibrational states of the first electronic excited state ($B^1\Sigma_u^+$) of the hydrogen molecule. The reaction suggested is a sequential energy transfer from the excited argon states through a photon to hydrogen singlet states which decay to ground state vibrationally excited states, according to:

$$e + Ar \rightarrow Ar\,(1s_4, 1s_2) \rightarrow Ar + h\nu \qquad (1)$$

followed by

$$h\nu + H_2 \rightarrow H_2\,(B\,^1\Sigma_u^+(v), C^1\Pi_u(v))$$

$$\rightarrow (X\,^1\Sigma_g^+(v'')) + h\nu' \qquad (2)$$

where $\nu \neq \nu'$. The argon states involved are dipole allowed and have large excitation cross sections in comparison with the metastable states.

Furthermore, the radiation is trapped in the discharge so excitation of hydrogen molecules may be the main loss process. Curran *et al* quote Lyman [4] and Takezawa *et al* [5] who observed resonance fluorescence in both the B→X and

$C \rightarrow X$ systems in an argon discharge operating between 0.1 and 10 Torr with a small admixture of hydrogen.

Vollmer *et al* [2] observed in a large radio frequency driven negative ion source the beneficial effect of 20% argon addition on the extracted negative ion current. Krypton and xenon admixtures have also been used but the resulting increase in H^- current density was much less than with argon.

Abate and Ramos [3] reported that the addition of 10% argon raised the negative ion current extracted from a magnetized sheet plasma by a factor of nine.

Source operation with a mixture of argon and hydrogen has been studied earlier by Leung *et al* [6]. They showed that there exists an optimum total pressure for each hydrogen base pressure. For a discharge power of 80 V, 3 A, the highest H^- output occurs at a total pressure of about 0.186 Pa. In this case the increase in H^- yield is 17% which is about the same percentage increase (18%) as in the plasma electron density in the extraction chamber.

The first objective of this work was to extend the work of Curran *et al*, to higher density plasma, by measuring the negative ion density by laser photodetachment in a magnetically confined and magnetically filtered dc filament discharge. Although our source is very similar to that of Curran *et al*, we did not exactly reproduce the features of this source, as evidenced by the difference in the observed plasma characteristics. The principal differences are in the position of the filaments and in the multipole magnetic field at the end flanges. In our source the filaments were located in the multicusp magnetic field close to the end flange. This field acted as a magnetic filter. In Ref. 1 the filaments were located in the field free region and there were no magnets on the end flanges.

The second objective of this work was to study the effect of argon additive on the extracted negative ion current from a small volume tandem H^- source, equipped with an external magnetic filter

A third objective of our work was to verify directly the assumption about the involved mechanism, Eq. 1 and 2, by recording the Werner and Lyman bands in the VUV and searching for the effect of argon additive. This region of the spectrum has been studied by numerous authors. Graham [7] effected this study in pure hydrogen in an effort to study the mechanism of hydrogen negative ion volume production. The VUV spectrum from mixtures of argon and hydrogen was studied by Fozza *et al* [8], in a microwave source at pressure from 1 to 10 Torr.

I. Experimental set-up and techniques.

The schematic diagram of the magnetically confined dc filament discharge is shown on Fig. 1 (see also Ref. 9). The discharge chamber is a stainless-steel vessel of 27 cm in length and 21 cm in diameter. Ten rows of ferrite magnets, surrounding the vessel, and four ferrite magnets on each end are arranged to produce a multicusp magnetic field for plasma confinement. The magnetic field is about 300 Gauss on the wall surface and a few Gauss at the center of the vessel. Two tungsten filaments attached to current feedthroughs located on the end plate generate primary electrons. They are located in the multicusp magnetic field, which acts as a magnetic filter. Therefore these electrons, which are accelerated by the applied discharge voltage to 100 eV, do not penetrate in the central plasma region, where the electron and negative ion densities are measured. Hydrogen and argon gas are admitted into the device through a port in the center of the end plate. The gas pressure is monitored by a Baratron gauge. The background pressure is measured with an ionization gauge.

The laser beam, 4 mm in diameter, is injected radially in the chamber. A cylindrical L-shaped probe is installed on a holder which is perpendicular to the laser beam. The probe is made of tungsten wire 25 mm in length and 0.15 mm in diameter. The probe is coaxial with the laser beam on a length of 15 mm. This probe is used for negative ion density measurement using photodetachment by a Nd YAG laser, and also for the measurement of the other plasma parameters. Details about the method of measurement of the negative ion density can be found in Ref. 9. The laser beam exits from the plasma chamber through a window located opposite to the extrance window.

The VUV-visible spectrophotometer ($30 \leq \lambda \leq 500$nm, 0.2 m focal length, Acton Research VM502, with a nominal resolution of 0.4 nm) has been connected to the plasma device through the flange where the laser exit window was usually located. A sliding valve was introduced to provide the possibility of performing photodetachment measurements in the presence of the VUV spectrophotometer. The latter is pumped independently of the plasma device by a turbomolecular pump, to less then 10^{-4} Pa. For studying the conditions when the pressure in the plasma chamber was $\geq$ 1 Pa, a 1 cm long collimation region with an internal diameter of 2 mm was introduced into the tube connecting the spectrophotometer to the plasma device.

In order to detect the VUV radiation we used a film of sodium salicylate deposited on glass to convert this radiation into visible one. To detect the converted light, we used a photo multiplier HAMAMATSU 721-01. The VUV spectrum was obtained in photon counting mode of the photomultiplier. The spectrum acquisition was made on a computer using a specially designed software with IEEE circuit.

In most studies, the discharge voltage was 100 V and the discharge current 1A. The measurement of the plasma parameters was completed before the installment of the VUV spectrophotometer.

The ion source used to study the effect of argon additive on the extracted negative ion current is shown on Fig. 2 (from Ref. 10). This compact ion source system was designed for positive ion beam formation, but we adapted it to negative ion extraction. The cylindrical ion source is 8 cm in diameter and 9 cm long. Twelve rows of samarium-cobalt magnets are attached on the copper side wall and produce the multicusp magnetic field. The mean field strength of each magnet is 1 T at the surface. In order to produce an external magnetic filter we added two ceramic magnets (5 cm long, with a magnetic field on the surface of 1 kGauss) outside the cylindrical side wall, perpendicular to the magnets forming the multicusp magnetic field.

The extraction system consists of three electrodes with 6-mm-diam holes: the plasma electrode, the lens electrode and the acceleration electrode, which is grounded. The source body is connected to the negative side of the acceleration power supply, while the voltage of the lens electrode, V_L, is adjusted to the optimum beam current. The negative ion component of the beam current is measured by a Faraday cup located downstream. A transverse magnetic field, installed at the entrance of the Faraday cup, rejects the electron component of the beam. An ionization gauge mounted on the source flange monitors the hydrogen and argon gas pressure in the ion source.

The source was operated dc, with 100 V - 1 A discharge. In order to obtain acceptable power loads on the acceleration and lens power supplies, we chose suitable plasma electrode bias (in the range +1 to +3 V), which reduced in certain limits the extracted electron current.

II.Results.

II.A. Effect of argon additive on the plasma parameters in the large source.

In order to effect the study of the effect of argon additive, we measured the pressure dependence of plasma parameters (electron density, negative ion density, electron temperature, plasma potential) on:

1. hydrogen pressure, in the range from 0.05 Pa to 1.5 Pa , and
2. argon additive pressure, for several values of the hydrogen base pressure, namely 0.05 Pa, 0.1 Pa, 0.5 Pa and 1 Pa.

A summary of these results is presented on Fig. 3. On each of the six graphs of this figure one compares the effect of hydrogen and argon additives versus the same total pressure, whether it is pure hydrogen or hydrogen plus argon additive.

The following observations can be made.

The electron density is increased more efficiently by adding argon, than by adding hydrogen. With the base hydrogen pressure of 0.05 and 0.1 Pa, increasing the total pressure by a factor of two, leads to an increase in electron density by a factor of three when argon is added. The effect of adding argon is lower when the base pressure is 0.5 Pa; the increase in electron density is only by a factor of two for a similar increase in total pressure. While the electron density goes up linearly in proportion to the argon pressure at low base hydrogen pressure (0.05 and 0.1 Pa), a saturation in the increase of the electron density is observed at higher initial pressure of hydrogen (0.5 and 1 Pa).

The electron temperature is essentially the same at the same total pressure in hydrogen and hydrogen with argon additive. This is particularly true at the low pressures studied. In the range 0.05 to 0.2 Pa the increase in total pressure leads to a reduction of the electron temperature. For pressures higher than 0.5 Pa, the electron temperatures are practically constant.

The plasma potential is systematically enhanced when the argon pressure is increased, while the increase of the hydrogen pressure leads to a reduction of the plasma potential. The floating potential smoothly goes up with pressure and has close values in hydrogen and hydrogen – argon mixture.

The difference between the plasma potential and floating potential also has close values in pure hydrogen and hydrogen - argon mixtures. This is a reasonable result, since this difference is related to the electron temperature, which is essentially the same, as noted above.

The negative ion density significantly goes up and attains a maximum when argon is added to low base hydrogen pressure (0.05 Pa, 0.1 Pa), but goes down when argon is added to higher initial hydrogen pressure (0.5 Pa, 1 Pa). Adding hydrogen to low base hydrogen pressure leads to an increase of the negative ion density. The optimum argon additive pressure is 40 to 60% of the base hydrogen pressure.

Comparing our observations to those of Curran *et al*, we can note the following:

• The observed increase in the negative ion density due to argon additive relative to that observed in pure hydrogen is lower in our experiment. Curran *et al* report an increase by a factor of 2.5 at 1 mTorr, when 20% to 40% of argon is added. The increase observed in our experiment is at most by a factor 1.5, when 40% of argon is added.

• The measured negative ion densities in pure hydrogen are much lower (a factor of ten) in the device of Curran *et al*, at similar pressure and discharge current. The negative ion densities vary in our device from 0.5×10^9 to 2×10^9 cm^{-3}. At 0.133 Pa, the negative ion density reported in Ref. 1 (Table 1) is 5.3×10^7 cm^{-3} while at this pressure in our device $n^- = 7 \times 10^8$ cm^{-3}.

• The electron temperature observed in our device is significantly lower than that reported by Curran *et al*: the maximum electron temperature is 1.5 eV in our device, but 4.5 eV in Ref. 1, for pure hydrogen. This is related to the presence of magnetic filtering in our device.

• The addition of argon does not change the electron temperature in our device at the same total pressure, but significantly lowers it in Ref. 1.

II.B. Effect of argon additive on the negative ion temperature.

The measurement of the duration of the photodetachment pulse provides the possibility to determine characteristic negative ion velocities and to estimate the negative ion temperature [11]. This possibility is related to the following: the theoretical model of laser-induced photodetachment of negative ions in plasma relies on the idea that the departure of an excess electron from the illuminated plasma column occurs when a negative ion from the surrounding plasma replaces it [12]. The decay of the probe electron current pulse is due to the arrival of negative ions into the probe collection region. As proposed by Devynck *et al* [11] it is possible to determine the velocity of the fastest negative ions, present in sizeable amounts, from the measurement of Δt_1 (time of the end of the plateau in the photodetachment electron current pulse):

$$v^-_{max} = (R - r_c) / \Delta t_1 \qquad (3)$$

where R is the radius of the laser beam and r_c is the radius of the probe collection region [13].

The total duration of the probe current pulse Δt_2 corresponds to the arrival of a group of slow H^- ions. From this characteristic time it is possible to determine another extreme velocity, v^-_{min} :

$$v^-_{min} = (R - r_c) / \Delta t_2 \qquad (4)$$

Another possibility, proposed by Nishiura *et al* [9], consists in determining the intermediate time after the laser pulse when the probe current is canceled first, before its inversion, Δt_o, and determining the average (thermal) negative ion velocity from the equation:

$$v_{th} = (R - r_c) / \Delta t_o \qquad (5)$$

We studied the effect of argon additive at three initial values of the hydrogen pressure: 0.05 Pa, 0.1 Pa and 1 Pa.

Figure 4 shows the photodetachment pulses in the plasma with base hydrogen pressure 0.05 Pa with various argon additives (from 0 to 80%). Note two important features: the continuous increase of the pulse amplitude with argon additive, which leads to the result shown on Figure 3b, and the increase of the pulse duration, which is analyzed in Figure 5.

Figure 5 presents the dependence on the pressure of the argon additive of three characteristic times: Δt_1, Δt_o and Δt_2. Figure 5 shows, for comparison, the variation of Δt_1, Δt_o and Δt_2 in the case when the additive is hydrogen. Note the linear increase of the times Δt_o and Δt_2 with the pressure of the argon additive, while Δt_1 remains constant. The hydrogen additive does not modify the value Δt_o and only slightly modifies Δt_2 .

Figure 6 shows the photodetachment electron current pulses in hydrogen plasma at 1 Pa with argon additive (from 0 to 50%). With this base hydrogen pressure the photodetachment pulse amplitude goes down with argon additive pressure (as also visible on Fig. 3b), and the pulse duration does not vary sensibly.

In order to calculate the various velocities from Eqs. 3-5, we have to calculate or measure the radius of the collection region, r_c. It was shown that r_c has the following expression:

$$r_c = r_p + A\ \Delta r_{sheath} \qquad (6)$$

with A in the range between two and three. r_p is the probe radius, Δr_{sheath} can be calculated using the theory by Kiel [14].

II.C. Search for the effect of argon additive in VUV spectra.

The study of the VUV spectra was performed in the large source (Fig. 1) in two different conditions:
(a) At low gas pressure (0.05 Pa and 0.1 Pa base hydrogen pressure) the VUV spectrometer was connected to the plasma chamber through a tube with the diameter 16 mm.
(b) For higher pressure (1 Pa base hydrogen pressure) the conductance between the VUV spectrometer and the plasma chamber was reduced by the introduction of a cylinder with an opening of 2 mm, 10 mm long.

The pressure in the duct between the VUV spectrometer and the source in these two conditions can be inferred from Table I. The pressure inside the VUV spectrometer was lower than the values indicated in Table I, due to its differential pumping and the presence of the spectrometer slit (10 μm) between the duct, where the ionization gauge was located, and the VUV spectrometer itself. These pressures are low enough to prevent absorption.

Figure 7 shows two examples of VUV spectra from pure hydrogen plasma and hydrogen plasma with argon admixture., with hydrogen base pressure 0.1 Pa (upper graph) and 0.05 Pa (lower graph). The discharge conditions were 100 V, 1A.

Table II presents the most intense lines in the VUV spectrum measured for a hydrogen discharge with a hydrogen pressure of 0.1 Pa. The discharge conditions were 100 V, 3 A. The Table II contains the measured wavelength values and the proposed identification for some of the observed lines. The identification is based on the comparison with data for H_2 singlet systems from [15]. The intensity of the various lines is also indicated. It can be noted that the spectrum contains four argon lines, the Lyman α, β, and γ lines of atomic hydrogen and Werner and Lyman system lines of molecular hydrogen.

Based on spectra similar to those of Fig. 7, we plotted in Fig. 8 the dependence on argon additive pressure of the intensity of Lyman α line and of a line of molecular hydrogen (Werner 0-2, according to our identification). The base hydrogen pressure was 0.1 Pa. For comparison, we also plotted the dependence of the intensities of these two lines on the pressure of hydrogen additive, with the same base hydrogen pressure. Note that the increase of the hydrogen pressure leads to the increase of both lines, while the addition of argon leads to the slight

reduction of the molecular line, and to a strong reduction of the Lyman α line, after attaining a maximum at 0.14 Pa.

The direct comparison of spectra in pure hydrogen and argon seeded discharge, at the same total pressure, observed with the initial hydrogen pressure of 0.05 Pa, 0.1 Pa and 1 Pa indicates that argon seeding does not enhance the intensity of any of the molecular lines recorded.

Figure 9 shows the dependence on argon additive pressure of the intensity of Lyman α line and of a line of molecular hydrogen (Werner 0-2) in the case when the base hydrogen pressure is 1 Pa. In this case the addition of argon leads to a strong reduction of both line intensities (> 50 %), while the addition of hydrogen leads to a small maximum in the intensity of the Lyman α line and the molecular line intensity stays at a constant level up to 1.4 Pa.

Thus our direct observation of the Werner and Lyman system lines in the VUV region does not support the assumption on the mechanism proposed by Curran et al [1] and expressed by Eqs. 1 and 2. We did not find any enhancement of the molecular Werner and Lyman system lines due to addition of argon to the hydrogen discharge. The Werner system lines correspond to the transitions from the singlet C state to the ground X state, while the Lyman system lines correspond to the transitions from the singlet B state to the ground X state..

II.D. Effect of argon additive on the extracted negative ion current from a small tandem H^- ion source.

The operation in pure hydrogen and in argon seeded hydrogen of the small tandem H^- ion source, shown on Fig. 2, have been compared. The rejection of the electrons by the transverse magnetic field of the Faraday cup was tested by operating the source with helium. No significant current to the Faraday cup was recorded in the case of helium operation.

We first measured the pressure dependence of the negative ion current in pure hydrogen. Fig. 10 shows that the I^- current attains a maximum of 67 μA at 6 mTorr.

The effect of adding argon is summarized on Fig. 11. A large increase in the extracted negative ion current was observed at hydrogen pressure below the optimum value: a factor of 3 increase in I^- was observed by adding 10 and 20% of

argon, when the base hydrogen pressure was 2 mTorr. A factor of 2 increase in I^- was observed when adding 13% of argon, when the base pressure was 3.2 mTorr. The negative ion current was reduced when adding argon at the base pressure of 6 mTorr. The relative variation of I^- versus argon/hydrogen ratio is shown on Fig. 12.

Thus the extracted negative ion current shows a large increase with argon mixing (a factor 2 to 3), when the base hydrogen pressure is well below the optimum value. This increase is larger than observed in the large H^- ion source by photodetachment, where the increase in negative ion density due to argon mixing a factor 1.5 at most. We assume that this is due to the fact that argon mixing reduces the negative ion temperature, as shown in Sec. II.B, and the ion-optical system is focalizing better the negative ion beam. This assumption has to be verified in future work.

III. Discussion and Conclusion.

As a result of the reported above experiments the main question to be answered is what determines the increase in H^- density and the increase in extracted H^- current, when argon is added to hydrogen in the ion source. It seams to us that the significant increase in electron density due to argon addition to hydrogen is the cause of the increase in negative ion density.

It is obvious from Fig. 3a that the electron density increase is larger when adding argon than when adding hydrogen. At first view this can be explained by at least three reasons:

(a) the three times larger ionization cross section for argon atom compared to that for hydrogen molecule, for an electron energy of 100 eV (9.24×10^{-17} cm^2 for hydrogen molecule, 2.85×10^{-16} cm^2 for argon).

(b) the 20 times larger mass of argon ions compared to the hydrogen molecular ions H_2^+, which, for the same thermal energy, leads to a 4.5 times longer wall loss time for argon ions, compared to hydrogen molecular ions.

c) the lower recombination loss of argon ions, compared to that of the hydrogen molecular ions. For the H_2^+ ions the dissociative recombination rate is much higher than the radiative recombination rate of argon ions.

A simple theoretical estimate of the electron density in the presence of a given argon additive fraction can be done for the condition of our experiment (*i.e.* wall loss of positive ions dominating), assuming that only monoenergetic primary electrons (100 eV) participate in the ionization of both hydrogen and argon. This assumption is justified at the lowest pressures studied. In the case of pure hydrogen the density of the secondary, plasma electrons is given by the following (Eq. 2 in [16]):

$$n_e = (L/v^+)\, n_p\, n_o\, \langle \sigma_i v_p \rangle \qquad (7)$$

Here n_p is the density of the primary electrons, L/v^+ is the positive ion lifetime for wall losses, $\langle \sigma_i v_p \rangle$ the reaction rate for ionization of H_2 by electron collisions, n_o - the density of neutral hydrogen molecules.

This estimate can be extended to the case of hydrogen with argon additive. The addition of argon leads to an increase of the electron density by a factor of 1+13.5 f, where f is the fraction of argon added to the initial hydrogen neutral density. This estimate takes into account the three times larger cross section of argon ionization compared to that of hydrogen and the 4.5 times longer wall loss time of argon ions, which is related to the mass ratio of Ar^+ and H_2^+ ions. The prediction from this estimate is much higher than the observed increase. For f=1 we observed an increase by a factor three at the lowest pressures studied (0.05 Pa and 0.1 Pa) and a factor two, at the pressure 0.5 Pa. The theoretical estimate gives an increase by a factor 14.5.

At the first view the difference between the observed increase in electron density and the simple theoretical estimate based on Eq. 7, could be due to the charge transfer reaction, converting the argon ions into molecular hydrogen ions (see Eq. 8). In this case the heavy argon ion would be replaced by the lighter hydrogen molecular ion which would have a shorter wall loss time. The electron density increase would take advantage in this case of the higher ionization cross section of argon, but not of his larger mass.

The charge transfer, Eq. 8, is not the only possible reaction in the argon-hydrogen mixture plasma. The reverse charge transfer reaction converting the H_2^+ ion into an Ar^+ ion (Eq. 10), and the ion-molecule reactions (9) and (11) leading to formation of ArH^+ ions, have also to be considered (see Ref. 17). Among these reactions, reaction (10) is endoergic and the rate depends on the vibrational state of the H_2^+ ion.

$$Ar^+ + H_2 \rightarrow H_2^+ + Ar, \qquad \Delta H = -0.31 \text{ eV} \qquad (8)$$

$$Ar^+ + H_2 \rightarrow ArH^+ + H \qquad \Delta H = -1.61 \text{ eV} \qquad (9)$$

$$H_2^+ + Ar \rightarrow H_2 + Ar^+ \qquad \Delta H = +0.31 \text{ eV} \qquad (10)$$

$$H_2^+ + Ar \rightarrow ArH^+ + H \qquad \Delta H = -1.30 \text{ eV} \qquad (11)$$

From the point of view of the positive ion wall loss, the formation of ArH^+ ions is not important, because its mass is very close to that of Ar^+. Unless its lifetime is very short, due to dissociative recombination, and in this case the positive ion loss will be enhanced by the formation of ArH^+ ions. However, although the recombination rate of ArH^+ ions has never been specifically measured, one expects that it would have a small recombination rate (less than 10^{-8} cm^3/s) as it does not have a curve crossing in the vicinity of v=0 level [18].

The cross section of the exothermic charge transfer reactions (8) leading to the formation of H_2^+ ions was reported by Baer et al [19] for the ion energy range 0.25 eV to 1.2 eV. At the lowest energy studied the cross section for this reaction is 3×10^{-16} cm^2. The cross section for the reaction (9) measured by the same authors at the same energy is 2.5×10^{-15} cm^2, i.e. 8 times larger.

The rate constant for reaction (9) at 300 K has been measured and is 1.1×10^{-9} cm^3/s (see [20]). From this rate constant we evaluate the cross section for reaction (9) to be 6×10^{-15} cm^2, at this low temperature (300 K), more relevant to our experiment.

Let us assume that at 0.25 eV the charge transfer cross section for reaction (8) is $\sigma_{ChX} = 3\times10^{-16}$ cm^2. The condition for the charge transfer loss to dominate over the wall loss is :

$$n_o(H_2) \geq (L\ \sigma_{ChX})^{-1} \qquad (12)$$

With the characteristic length L = 20 cm, we find $n_o(H_2) \geq 1.6\times10^{14}$ cm^{-3}, or $P(H_2)$ = 0.66 Pa. It follows that charge transfer, Eq. 8, can be neglected at the studied pressures, 0.1 and 0.05 Pa.

Let us consider the much faster proton transfer reaction (9). The condition for Ar^+ ion loss due to this reaction to dominate over the wall loss is as follows:

$$n_o(H_2) \geq (v^+_{Ar}/L\langle\sigma v\rangle_{PT}) \qquad (13)$$

With $\langle\sigma v\rangle_{PT}=1.1\times10^{-9}$ cm^{-3} (see Ref. 20), we find $n_o(H_2) = 1.8\times10^{12}$ cm^{-3} or $P(H_2)$ $=7\times10^{-3}$ Pa. Thus for the lowest pressure studied by us, 0.05 Pa, the proton transfer dominates over the wall loss. This could explain why the observed increase of the electron density is lower than that predicted by the simple model, if the recombination rate of ArH^+ were large. But this does not seem to be the case, as shown above.

It could also be questioned what is the role of ArH^+ ions, and whether their presence has some impact on negative hydrogen ion formation.

The negative ion density is proportional to the electron density, due to the negative ion formation by dissociative electron attachment, which implies a low energy electron and a rovibrationally excited molecule:

$$e + H_2(v'') \rightarrow H^- + H \qquad (14)$$

The higher vibrational states are populated by radiative decay from singlet electronic states excited by collisions of ground state molecules with energetic primary electrons, i.e. the reaction:

$$e + H_2(X\ ^1\textstyle\sum_g^+,\ v'' = 0) \rightarrow e + H_2^*\ (B\ ^1\textstyle\sum_U^+,\ C\ ^1\Pi_u\ ...) \qquad (15)$$

$$H_2^* (B\,^1\Sigma_U^+ , C\,^1\Pi_u \ldots) \rightarrow H_2 (X\,^1\Sigma_g^+, v'') + h\nu \qquad (16)$$

This process is designated as E-V excitation, to indicate that vibrational excitation is produced by high energy electrons.

The argon mixing modifies the low energy electron density, but does not affect the density of rovibrationally excited molecules. This was proved by our study of the VUV spectra, showing that no increase in the formation of such molecules occurs when mixing argon. We conclude that in pure hydrogen there are not enough low energy electrons for an efficient use of the rovibrationally excited molecules.

We have shown that the negative ion temperature is lowered by the argon mixing to hydrogen. In view of the importance of this observation, we will pursue its study by the two-laser technique.

The hypothesis proposed in Ref. 1 that the population of vibrational levels is enhanced due to argon mixing was not confirmed in our study of the VUV spectrum. Other ways to enhance negative ion production when argon is mixed to hydrogen will be considered, in addition to the enhancement of the electron density.

References.

1.N.P. Curran, M.B. Hopkins, D. Vender and B.W. James, Plasma Sources Sci. Technol., **9**, 169 (2000)

2.O. Vollmer, H. Falter, P. Frank, B. Heinemann, W. Kraus, P. Massmann, P. McNeely, R.Riedl, E. Speth, R. Trainham and R. Wilhelm, Rev. Sci. Instrum., **71**, Nb 2, 939 (2000)

3. Yohannes Abate and Henry J. Ramos, Rev. Sci. Instrum., **71**, Nb 10, 3689 (2000)

4. T. Lyman, Astrophys. J., **33**, 98 (1911)

4. S. Takegawa, F.R. Innes and Y. Tanaka, J. Chem. Phys., **45**, 2000 (1966)

5. K.N. Leung, K.W. Ehlers and R.V. Pyle, Rev. Sci. Instrum., **56**, 2097 (1985)

6. W.G. Graham, J. Phys. D: Appl. Phys., **17**, 2225 (1984)

7. A.C. Fozza, A. Kruse, A. Hollander, A. Ricard and M.R. Wertheimer, J. Vac. Sci. Technol. A **16**, 72 (1988)
8. M. Nishiura, M. Sasao and M. Bacal, J. Appl. Phys., 83, Nb 6, 2944 (1998)

9. M. Nishiura, M. Sasao, M. Wada, M. Hamabe, T. Kuroda and S.K. Guharay, Rev. Sci. Instrum., **71**, Nb 2, Part II, 1171 (2000)

11. P. Devynck, J. Auvray, M. Bacal, P. Berlemont, J. Bruneteau, R. Leroy and R.A. Stern, Rev. Sci. Instrum., **60**, 2873 (1989)

12. R.A. Stern, P. Devynck, M. Bacal, P. Berlemont, and F. Hillion, Phys. Rev. A, **41**, 3307 (1990)

13. M. Bacal, Plasma Sources Sci. & Technol., **2**, 190 (1993) (see Eqs. 10 and 11)

14. R.E. Kiel, AIAA J., **6**, 708 (1968)

15. Spectroscopic Data. vol. 2. Homonuclear Diatomic Molecules. Edited by S.N. Suchard and J.E. Melzer, p. 194.

16. M. Bacal, A.M. Bruneteau and M. Nachman, J. Appl. Phys., **55**, 15 (1984)

17. F.A. Houle, S.L. Anderson, D. Gerlich, T. Turner, Y.T. Lee, J. Chem. Phys., **77**, 748 (1982)

18. J. Brian A. Mitchell, Private communication (2001)

19. M. Baer, C.-L. Liao, R. Xu, G.D. Flesch, S. Nourbakhsh, C.Y. Ng, J. Chem. Phys., **93**, 4845 (1990)

20. F.C. Fehsenfeld, E.E. Ferguson and A.L. Schmeltekopf, J. Chem. Phys., **45**, 404 (1966)

Figure captions.

Figure 1. Illustration of multicusp ion source, with laser and probe for photodetachment measurements of negative ion density.

Figure 2. Multicusp ion source and beam extraction system.

Figure 3. Dependence of plasma parameters on the total pressure, for the case of pure hydrogen additive (open symbols) and for the case of argon additive (closed symbols). Four base hydrogen pressures were studied (0.05, 0.1, 0.5 and 1 Pa).

Fig. 4. Photodetachment electron current pulses in hydrogen plasma at 0.05 Pa with argon additive (from 0 to 80%). Discharge voltage 100 V, discharge current 1 A.

Fig. 5. Variation of recovery times Δt_1 , Δt_o and Δt_2 with argon additive(closed symbols) and hydrogen additive (open symbols) pressure, for a base hydrogen pressure of 0.05 Pa.

Fig. 6. Photodetachment electron current pulses in hydrogen plasma at 1 Pa with argon additive (from 0 to 50%). Discharge voltage 100 V, discharge current 1 A.

Fig. 7. VUV spectrum from pure hydrogen discharge and H_2 + Ar mixture plasma. Upper graph : base hydrogen pressure 0.1 Pa. Lower graph : base hydrogen pressure 0.05 Pa.

Fig. 8. Dependence on argon additive pressure of the intensity of Lyman _ line and of the line of molecular hydrogen at 110.016 nm. The base hydrogen pressure was 0.1 Pa. The discharge conditions are 100 V, 1 A. For comparison, we also plotted the dependence of the intensities of these two lines on the pressure of hydrogen additive, with the same initial hydrogen pressure.

Fig. 9. Dependence on argon additive pressure of the intensity of Lyman_ line and of the line of molecular hydrogen at 110.016 nm in the case when the initial hydrogen pressure is 1 Pa. The discharge conditions are 100 V, 1 A. For comparison, we also plotted the dependence of the intensities of these two lines on the pressure of hydrogen additive, with the same base hydrogen pressure.

Fig. 10. Pressure dependence of the extracted negative ion current in pure hydrogen discharge (closed circles) and in H_2 + Ar mixture discharge (open circles). The hydrogen pressure is fixed at 0.27, 0.43 and 0.81 Pa, when argon is admixed with hydrogen. 100 V, 1 A discharge.

Fig. 11. Relative increase of the negative ion current versus argon/hydrogen ratio.

Table I.

Pressure in the ion source (Column 1) and pressure in the duct between the VUV spectrometer and the source (Column 2 and Column 3). In Column 2 corresponds to condition (a) (16 mm diameter diaphragme), while Column 3 corresponds to condition (b) (tube 2 mm diameter, 10 mm long) described in Sec. II.C.

Pressure in ion source	Pressure in duct (reading of Ionization Gauge)	
	Condition (a)	Condition (b)
Pa	Pa	Pa
0.1	1.9×10^{-3}	3.9×10^{-2}
0.5	8.1×10^{-3}	
1.0	1.7×10^{-2}	
1.6	2.7×10^{-2}	

Table II.

Measured and correct (from Ref. 15) wavelengths of lines in the spectrum of H_2 discharge and their identification. Experimental conditions : Discharge voltage 100 V, discharge current 3 A, Hydrogen pressure 0.1 Pa. Entrance slitwidth : 5 μm. Exit slitwidth : 5 μm.

I Counts/s (arbitrary. units)	Wavelength (as measured) nm		Wavelength (from Ref. 15) nm
0,01155465	91,9756097	Argon	91.978
0,00570715	93,2456445	Argon	93.226
0,00921565	93,351480		
0,01568688	97,2321428	H Lyman gamma	97.29
0,02983003	102,629790	H Lyman beta	102.637
0,01337907	104,746515	Werner 2-2 andArgon	104.73
0,01033837	106,334059	Argon	106.33
0,04113519	109,932491	Werner 0-2	109.89
0,04863558	110,038327		
0,04101044	111,696428	Werner 1-3	111.58
0,04442538	114,554006	Werner 0-3	114.54
0,04450335	114,695122		
0,01981912	115,224303		
0,01883674	115,294861		
0,01571807	115,471254		
0,05816311	116,212108	Werner 1-4	116.08
0,0343521	116,776568		
0,05167628	117,587979	Werner 2-5	117.54
0,0572431	117,658537		
0,03881179	118,152439	Lyman 5-3	118.12
0,02137845	118,646342		
0,03301107	118,858014	Werner 3-6	118.89
0,04009044	119,069686		
0,03296429	119,316638		
0,02922189	120,198606	Werner 4-7	120.13
0,04745049	120,692509	Werner 1-5	120.62
0,02169032	121,045296		
0,02474661	121,292247		
1	121,680314	H Lyman Alpha	121.5
0,02256354	122,456446		
0,04295961	123,020906	Werner 3-7	122.96
0,02588492	123,303136		
0,02981444	123,867596		
0,0390145	123,973432	Werner 4-8	123.92

0,02491814	124,185105	Lyman 13-7	124.28
0,02463746	124,4673345	Lyman 10-6	124.44
0,02997037	124,679007	Lyman 7-5	124.67
0,03444566	124,855401	Lyman 4-4	124.98
0,02806799	125,137631		
0,04548573	125,490418	Lyman 1-3	125.41
0,04147825	125,737369	Lyman 12-7	125.74
0,03046936	126,0901568	Lyman 9-6	126.04
0,03238734	126,301829		
0,02354592	126,866289	Lyman 8-6	126.86
0,03823484	127,077962		
0,02379542	127,466028	Lyman 0-3	127.52
0,04341182	127,748258		
0,04341182	127,748258		
0,02766256	128,347997	Lyman 13-8	128.33
0,01376891	129,441638		
0,01604553	133,463415	Lyman 0-4	133.42
0,02137845	133,60453		
0,02072353	133,88676		
0,01941369	134,310105	Lyman 7-7	134.38
0,02507407	134,486498		
0,01922657	134,662892	Lyman 2-5	134.57
0,02190862	134,73345		
0,01687198	134,980401		
0,01880555	135,403746		
0,02820833	135,862369		
0,0235927	136,003484		
0,01585841	137,23824		
0,01766724	137,414634		
0,02098862	137,8027	Lyman 3-6	137.85
0,01638859	138,190767		
0,02357711	139,49608	Lyman 0-5	139.45
0,02158116	140,34277	Lyman 2-6	140.26
0,01863402	143,412021	Lyman 3-7	143.34
0,01980352	143,517857		
0,03305785	143,694251	Lyman 5-8	143.65
0,01811944	146,939896		
0,02069234	147,716028		
0,02201778	148,77439	Lyman 3-8	148.77
0,01919538	148,986063		
0,03042258	149,656359		
0,02301575	151,737805	Lyman 0-7	151.71

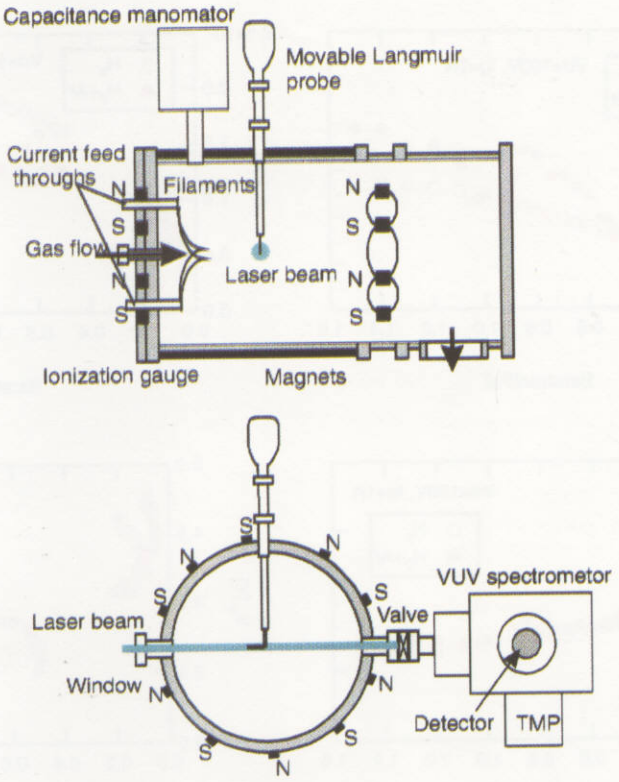

Fig.1 Illustrations of multicusp ion source and probe.

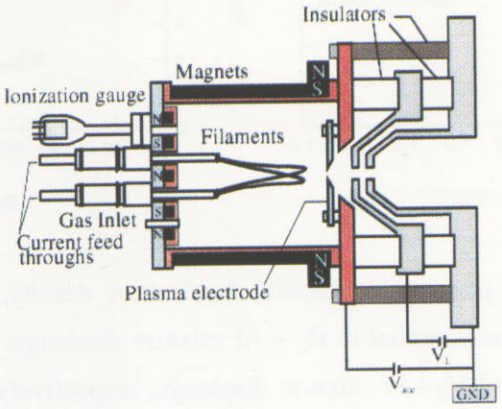

Fig.2 Illustrations of multicusp ion source.

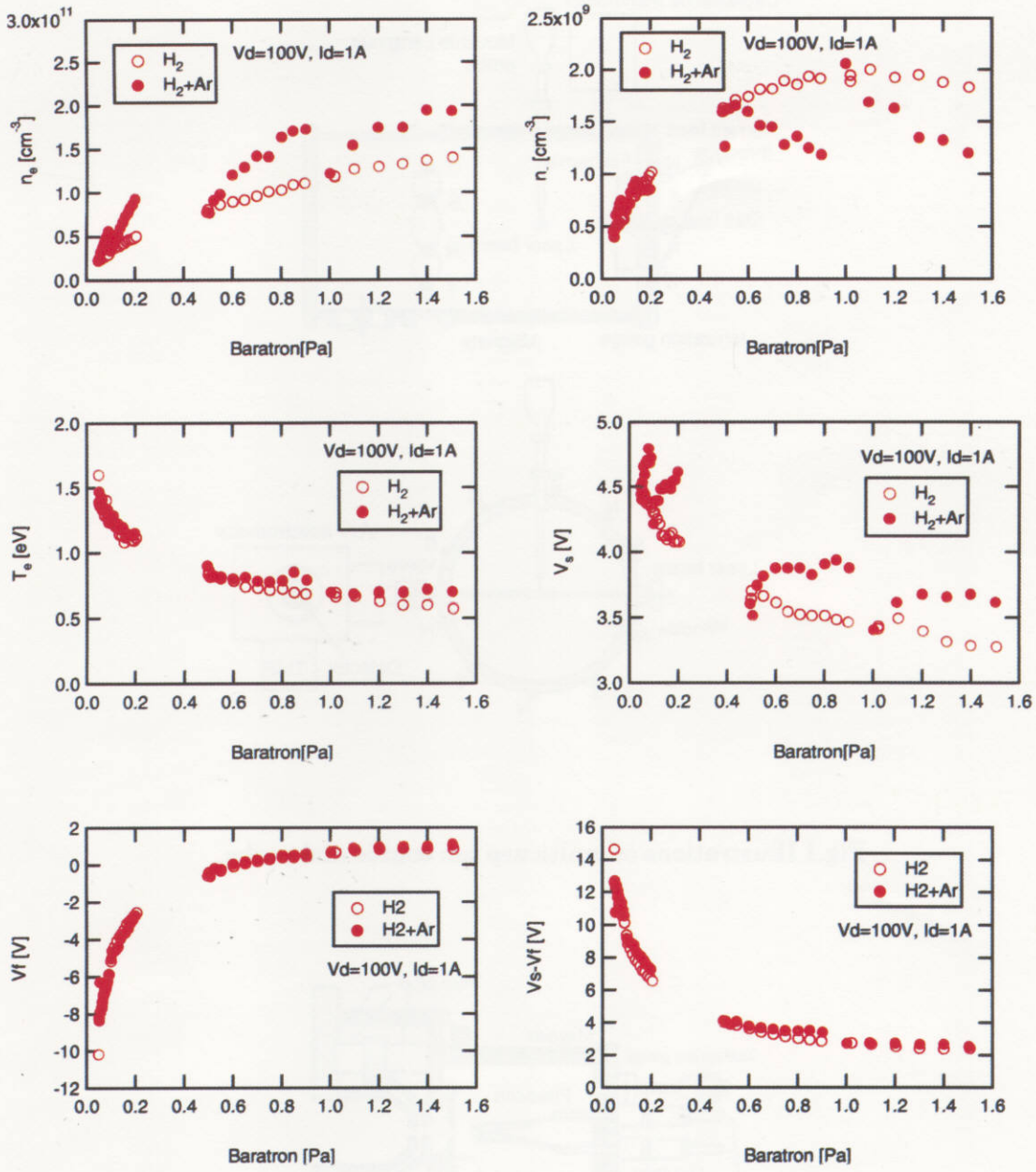

Fig.3 Characteristics of plasma parameters, (a)electron density, (b)H^- density, (c)electron temperature, and (d)plasma potential in H_2 + Ar mixture discharge. Closed circle and open one show the H_2 discharge and H_2 +Ar mixture discharge, respectively. The hydrogen pressure is fixed at 0.05, 0.1, 0.5, and 1.0 Pa, when argon gas is admixed with hydrogen gas. The discharge conditions are V_d = 100V, and I_d = 1A.

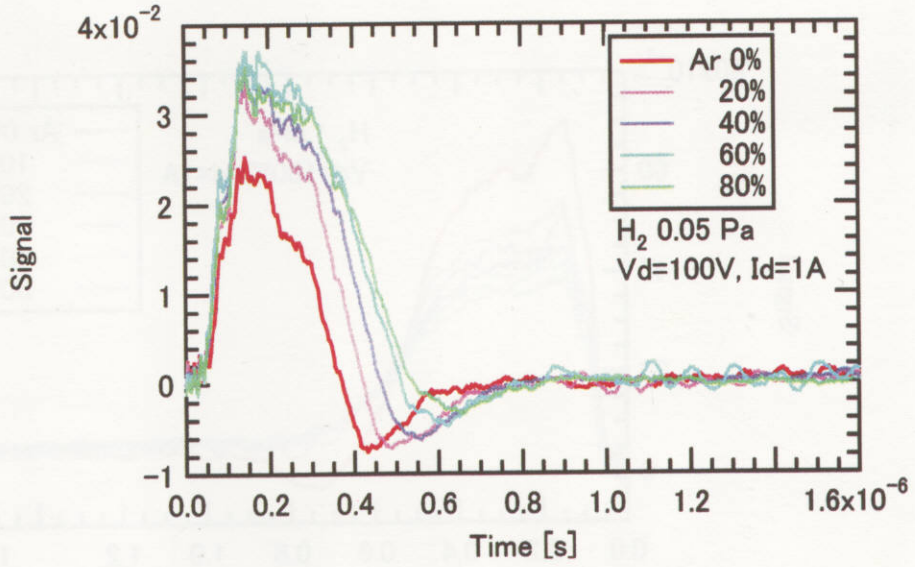

F ig. 4. Photodetachment electron current pulses in hydrogen plasma at 0.05 Pa with argon additive (from 0 to 80%). The discharge conditions are V_d=100V, and I_d=1A.

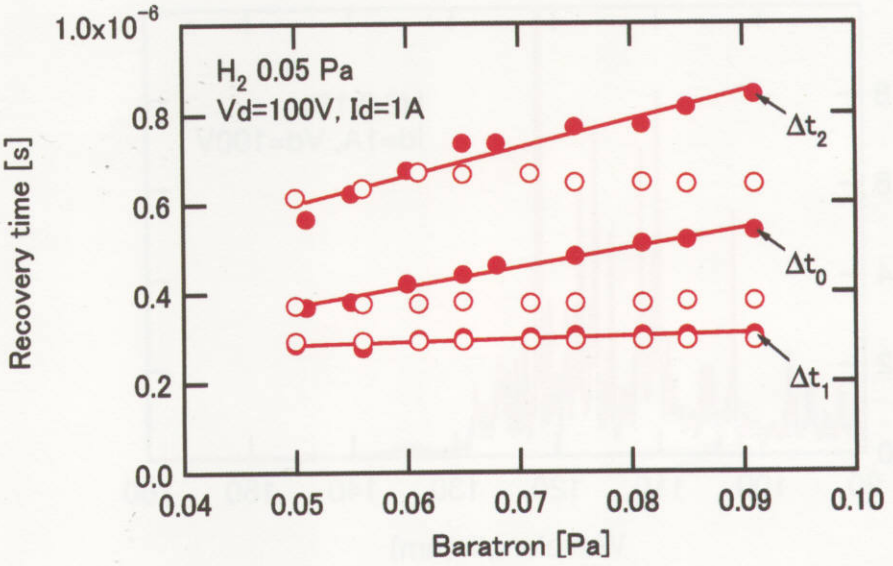

Fig. 5 Variation of recovery times Δt_1, Δt_0, and Δt_2, with argon additive (closed symbols) and hydrogen additive (open symbols) pressure, for a base hydrogen pressure of 0.05 Pa

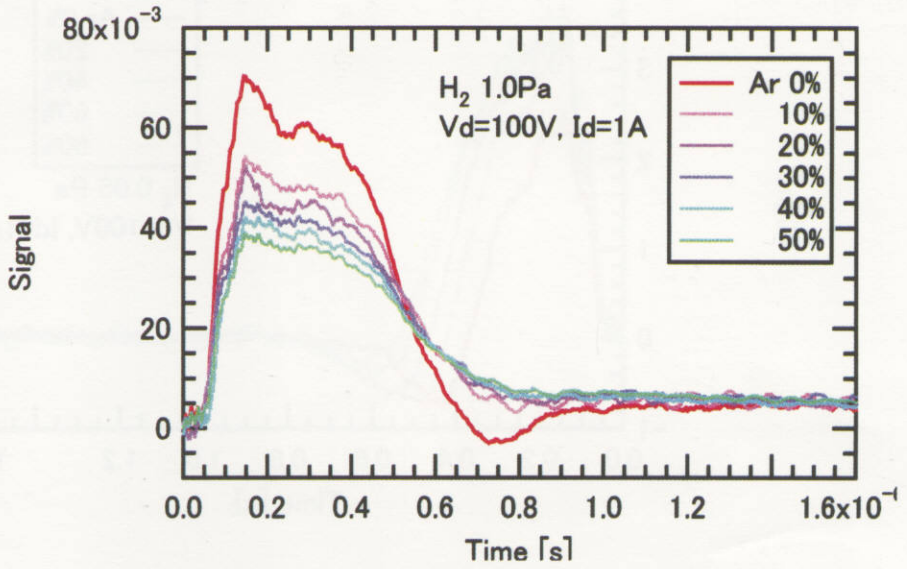

Fig.6 Photodetachment electron current pulses in hydrogen plasma at 1 Pa with argon additive (from 0 to 50%). Discharge voltage 100V, discharge current 1A.

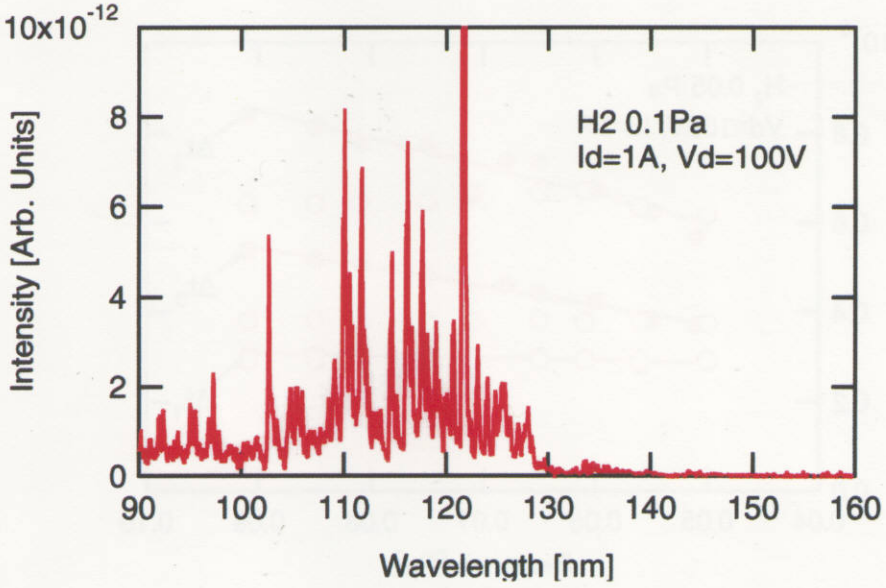

Fig. 7 VUV spectrum from pure hydrogen discharge and H_2 + Ar

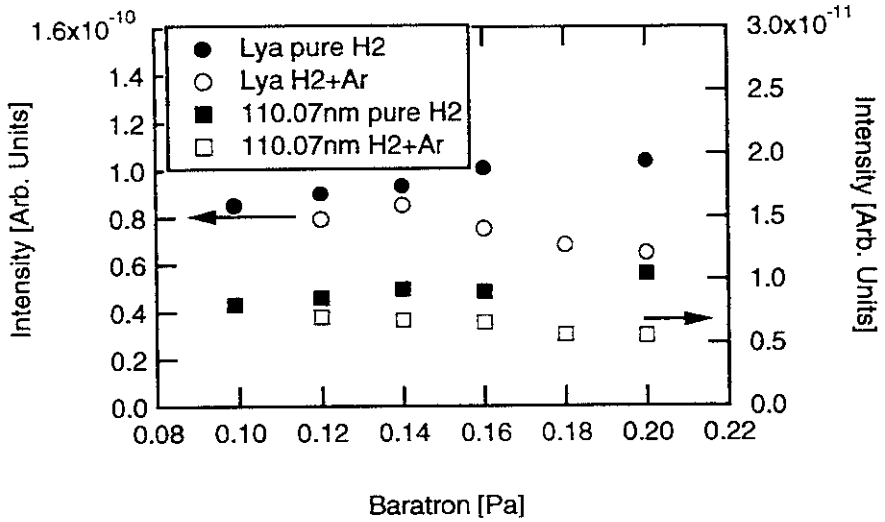

Fig. 8 Dependence on argon additive pressure of the intensity of Lyman a line and of the line of molecular hydrogen at 110.016 nm. He base hydrogen pressure was 0.1 Pa. The discharge conditions are 100V, 1A. For comparison, we also plotted the dependence of the intensities of these two lines on the pressure of hydrogen additive with the same initial hydrogen pressure.

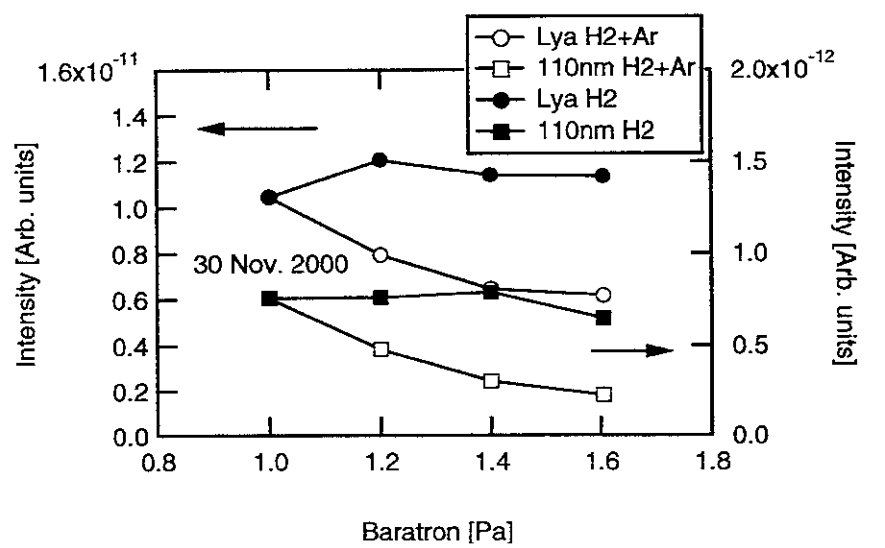

Fig. 9 Dependence on argon additive pressure of the intensity of Lyman a line and of the line of molecular hydrogen at 110.016 nm. He base hydrogen pressure was 1 Pa. The discharge conditions are 100V, 1A. For comparison, we also plotted the dependence of the intensities of these two lines on the pressure of hydrogen additive with the same initial hydrogen pressure.

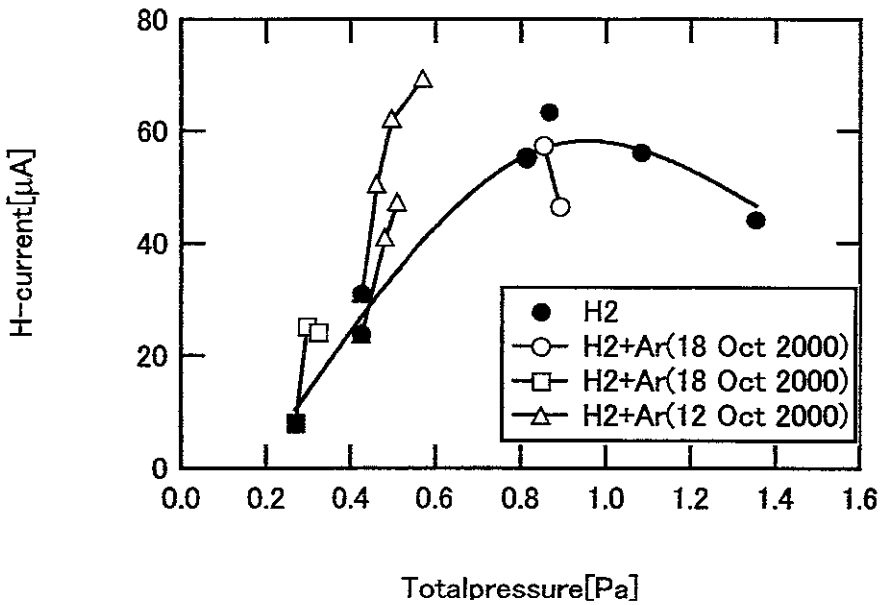

Fig. 10 Pressure dependence of the extracted negative ion current in pure hydrogen discharge (closed circles) and in H2 ; Ar mixture discharge (open circles). The hydrogen pressure is fixed at 0.27, 0.43, and 0.81 Pa, when argon is admixed with hydrogen. The discharge conditions are 100V, 1A.

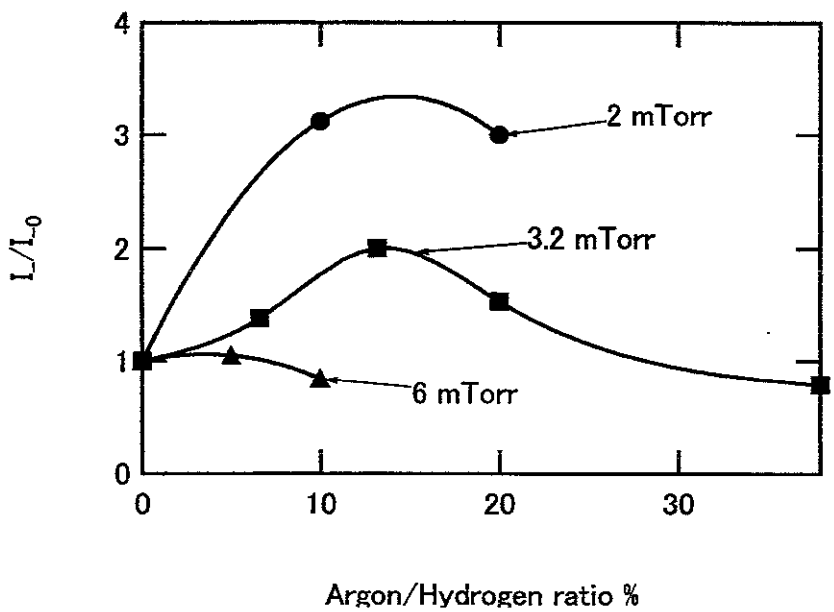

Fig. 11 Relative increase of the negative ion current versus argon.hydrogen ratio.

Recent Issues of NIFS Series

NIFS 684 S Kida and S Goto
Line Statistics Stretching Rate of Passive Lines in Turbulence Mar 2001

NIFS 685 R Tanaka, T Nakamura and T Yabe,
Exactly Conservative Semi-Lagrangian Scheme (CIP-CSL) in One-Dimension Mar 2001

NIFS-686 S Toda and K. Itoh,
Analysis of Structure and Transition of Radial Electric Field in Helical Systems Mar 2001

NIFS-687 T Kuroda and H Sugama,
Effects of Multiple-Helicity Fields on Ion Temperature Gradient Modes Apr 2001

NIFS-688 M Tanaka,
The Origins of Elctrical Resistivity in Magnetic Reconnection Studies by 2D and 3D Macro Particle Simulations Apr 2001

NIFS-689 A Maluckov, N Nakajima, M Okamoto, S Murakami and R Kanno,
Statistical Properties of the Neoclassical Radial Diffusion in a Tokamak Equilibrium Apr 2001

NIFS-690 Y Matsumoto, T Nagaura, Y Itoh, S-I Oikawa and T Watanabe,
LHD Type Proton-Boron Reactor and the Control of its Peripheral Potential Structure Apr 2001

NIFS-691 A Yoshizawa, S -I. Itoh, K Itoh and N Yokoi,
Turbulence Theories and Modelling of Fluids and Plasmas Apr 2001

NIFS-692 K Ichiguchi, T Nishimura, N Nakajima, M Okamoto, S -i Oikawa, M Itagaki,
Effects of Net Toroidal Current Profile on Mercier Criterion in Heliotron Plasma Apr 2001

NIFS-693 W Pei, R. Horiuchi and T Sato,
Long Time Scale Evolution of Collisionless Driven Reconnection in a Two-Dimensional Open System Apr 2001

NIFS-694 L.N Vyachenslavov, K Tanaka, K Kawahata,
CO2 Laser Diagnostics for Measurements of the Plasma Density Profile and Plasma Density Fluctuations on LHD Apr 2001

NIFS-695 T Ohkawa,
Spin Dependent Transport in Magnetically Confined Plasma May 2001

NIFS-696 M Yokoyama, K. Ida, H. Sanuki, K Itoh, K Narihara, K Tanaka, K Kawahata, N Ohyabu and LHD experimental group
Analysis of Radial Electric Field in LHD towards Improved Confinement May 2001

NIFS-697 M Yokoyama, K Itoh, S Okamura, K Matsuoka, S -I Itoh,
Maximum-J Capability in a Quasi-Axisymmetric Stellarator May 2001

NIFS-698 S-I Itoh and K Itoh,
Transition in Multiple-scale-lengths Turbulence in Plasmas May 2001

NIFS-699 K. Ohi, H Naitou, Y Tauchi, O. Fukumasa,
Bifurcation in Asymmetric Plasma Divided by a Magnetic Filter May 2001

NIFS-700 H Miura, T Hayashi and T Sato,
Nonlinear Simulation of Resistive Ballooning Modes in Large Helical Device June 2001

NIFS-701 G Kawahara and S Kida,
A Periodic Motion Embedded in Plane Couette Turbulence: June 2001

NIFS-702 K. Ohkubo,
Hybrid Modes in a Square Corrugated Waveguide June 2001

NIFS-703 S -I Itoh and K Itoh,
Statistical Theory and Transition in Multiple-scale-lengths Turbulence in Plasmas June 2001

NIFS-704 S Toda and K Itoh,
Theoretical Study of Structure of Electric Field in Helical Toroidal Plasmas June 2001

NIFS-705 K Itoh and S-I Itoh,
Geometry Changes Transient Transport in Plasmas. June 2001

NIFS-706 M. Tanaka and A. Yu Grosberg
Electrophoresis of Charge Inverted Macroion Complex Molecular Dynamics Study: July 2001

NIFS-707 T-H Watanave, H Sugama and T Sato
A Nondissipative Simulation Method for the Drift Kinetic Equation July 2001

NIFS-708 N Ishihara and S Kida,
Dynamo Mechanism in a Rotating Spherical Shell Competition between Magnetic Field and Convection Vortices July 2001

NIFS-709 LHD Experimental Group.
Contributions to 28th European Physical Society Conference on Controlled Fusion and Plasma Physics (Madeira Tecnopolo, Funchal, Portugal, 18-22 June 2001) from LHD Experiment July 2001

NIFS-710 V Yu. Sergeev, R.K. Janev, M.J Rakovic, S. Zou, N Tamura, K V Khlopenkov and S Sudo
Optimization of the Visible CXRS Measurements of TESPEL Diagnostics in LHD, Aug 2001

NIFS-711 M. Bacal, M. Nishiura, M Sasao, M Wada, M. Hamabe, H Yamaoka,
Effect of Argon Additive in Negative Hydrogen Ion Sources; Aug 2001